ELSEVIER

Contents lists available at ScienceDirect

International Journal of Particle Therapy

journal homepage: www.sciencedirect.com/journal/ijpt



NTCP-Based Prediction of Lung Sparing With IMPT in BC Patients and Implication of Patient Selection



Xiao-Yu Wu $(MD)^{1,2,\#,\$}$, Mei Chen $(MS)^{1,2,\#}$, Gang Cai $(MD)^{1,2}$, Rong Cai $(MD)^{1,2}$, Cheng Xu $(MD)^{1,2}$, Dan Ou $(MD)^{1,2}$, Fei-Fei Xu $(MD)^{1,2}$, Yu-Jie Wang $(MD)^{1,2}$, Huan Li $(MD)^{1,2}$, Min Li $(PhD)^{1,2}$, Yi-Bin Zhang $(BS)^{1,2}$, Lu Cao $(MD)^{1,2,*}$, Jia-Yi Chen $(MD)^{1,2,*}$

ARTICLE INFO

Keywords:
Breast cancer
Thoracic anatomical features
Patient selection for proton therapy
NTCP model
Radiation-induced lung injury

ABSTRACT

Purpose: To compare the difference in normal tissue complication probability (Δ NTCP) between proton therapy (PT) and photon therapy plans using radiation-induced lung injury (RILI) as an endpoint and to analyze its correlation with thoracic anatomic features in breast cancer patients.

Materials and Methods: A total of 409 breast cancer patients receiving photon intensity-modulated radiation therapy were randomly split into training and testing sets at an 8:2 ratio. A dose-modifying-factors (DMFs)-incorporated Lyman-Kutcher-Burman NTCP model was developed by maximum likelihood estimation with the training set to predict the risk of grade ≥ 1 RILI (CTCAE 5.0) within 1 year after radiotherapy. The DMFs stood for baseline risk factors were identified by least absolute shrinkage and selection operator regression and unimultivariable logistic regression. After model validation, PT plans were generated for 80 patients from the dataset. The Pearson/Spearman rank correlation coefficient followed by linear regression was used to assess the correlation between anatomic features and lung Δ NTCP between photon and proton plans.

Results: BMI ≥ 23.52 kg/m² (P = .049) and interval between last cycle of chemotherapy and radiotherapy (ICR) ≤ 20 days (P = .014) were found to be independent risk factors for RILI. The optimal NTCP parameters were: n = 0.40, m = 0.22, TD50 = 24.66Gy, DMF-BMI = 0.88, and DMF-ICR = 0.92. The model performed well in area under the receiver operating curve (training set 0.754, testing set 0.733) and other validation tests. Among the 80 patients with photon and proton plans, the mean Δ NTCP was 57.45% \pm 10.51%. Linear regression showed a significant positive correlation between Arc Height to Base Ratio at the transverse plane of the sternal angle and Δ NTCP (regression coefficient 56.56, P = .049).

Conclusion: BMI $\geq 23.52 \text{ kg/m}^2$ and ICR ≤ 20 days are risk factors for RILI. In patients with larger Arc Height to Base Ratio at the transverse plane of the sternal angle, PT plans suggest greater lung sparing in comparison to intensity-modulated radiation therapy. Further studies are needed to validate this association.

¹ Department of Radiation Oncology, Ruijin Hospital, Shanghai Jiao Tong University, School of Medicine, Shanghai, China

² Shanghai Key Laboratory of Proton-therapy, Shanghai, China

Abbreviations: PT, proton therapy; NTCP, normal tissue complication probability; NIPP, national indication for protocol proton therapy; BC, breast cancer; ACE, acute coronary event; RILI, radiation-induced lung injury; OAR, organ at risk; DMF, dose modifying factor; LKB, Lyman–Kutcher–Burman; DVH, dose-volume histogram; IMRT, intensity-modulated radiation therapy; CT, computed tomography; EUD, equivalent uniform dose; LL, log-likelihood; CI, confidence interval; LASSO, least absolute shrinkage and selection operator; AUC, area under the receiver operating curve; CTV, clinical target volume; IMPT, intensity-modulated proton therapy; RBE, relative biological effectiveness; AP, anterior-posterior; LR, left-right; AHBR, arc height to base ratio; ROC, receiver operating curve; BMI, body mass index; ISR, interval between surgery and radiotherapy; ICR, interval between last cycle of chemotherapy and radiotherapy; STD, standard deviation; RP, radiation pneumonitis; MLD, mean lung dose; DIBH, deep-inspiration breath-hold; RNI, regional nodes irradiation; FB, free-breathing

^{*} Corresponding authors. Department of Radiation Oncology, Ruijin Hospital, Shanghai Jiao Tong University, School of Medicine, 197 Ruijin Er Road, Shanghai, 200025, China.

E-mail addresses: wxy01m68@rjh.com.cn (X.-Y. Wu), cl11879@rjh.com.cn (L. Cao), cjy11756@rjh.com.cn, chenjiayi0188@aliyun.com (J.-Y. Chen).

Shared first authors.

^{\$} Author responsible for statistical analysis.

Introduction

Although the number of proton facilities is growing worldwide, due to its hitherto limited resources and high expenses, optimizing patient selection, especially in high incidence disease such as breast cancer (BC), so as to make the best use of the available resources is currently a topic of interest. For example, in the Netherlands, a model-based approach based on normal tissue complication probability (NTCP) models has been attempted for determining the national indication protocol for proton therapy (NIPP), including head and neck cancers and BC, in which the BC recommendation was based on a 2% or higher risk reduction of acute coronary event (ACE) using the Darby model with proton therapy (PT) compared to photons. However, other important radiation toxicity following BC radiotherapy, such as radiation-induced lung injury (RILI), remains underrecognized despite its clinical significance.

The NTCP model-based approach may cause extra workload, as it necessitates both photon and proton treatment planning for each patient. 2,3 Anatomical features have been summarized to estimate the dose to certain organs at risk (OARs). Stahl et al⁷ found that the degree of pectus excavatum assessed by the Haller Index was positively correlated with the mean heart dose (P < .001) in BC patients.

For the purpose of quantifying the benefit of PT in terms of lung toxicity while foregoing treatment planning comparison, in this study, we developed a dose-modifying-factors (DMFs)-incorporated Lyman–Kutcher–Burman (LKB)-NTCP model to predict the risk of RILI after postoperative BC radiotherapy. Based on the model, we tried to identify thoracic anatomic features that correlate with the benefit of PT in terms of lung protection (assessed by the Δ NTCP between proton and photon plans) and to provide references for patient selection.

Materials and methods

NTCP model development

Patient enrollment and data collection

A total of 409 BC patients with complete baseline characteristics, dose-volume histograms (DVHs), and follow-up results for RILI from two prospective clinical trials (clinicaltrials.gov #NCT02942615, #NCT03829553) who underwent postoperative radiotherapy at Ruijin Hospital, Shanghai Jiao Tong University, School of Medicine during August 2017 to February 2022 were retrospectively enrolled for this study. All patients received intensity-modulated radiation therapy (IMRT) for chest wall or whole breast with or without regional lymph node [supraclavicular \pm axillary \pm internal mammary lymph node] at a prescription dose of 40.05 or 50 Gy in 15 or 25 fractions, with or without a tumor bed boost of 10 to 16 Gy in 4 to 8 fractions. The DVHs and other dose-volume metric data of the ipsilateral lung were collected after being translated into equivalent dose in 2-Gy fractions at a α/β value of 3^{8} for later analysis. The dataset was then randomly divided into a training set and a testing set in an 8:2 ratio.

The endpoint event was defined as grade ≥ 1 RILI (graded according to the Common Toxicity Criteria for Adverse Events version 5.0^{9}) within 1 year after the completion of radiotherapy. Asymptomatic grade 1 RILI is defined as lung density changes in the region adjacent to the irradiated target. All RILI diagnoses were based on computed tomography (CT) scans after completion of radiotherapy and were independently reviewed and approved by an external senior radiology expert.

NTCP modeling

The case data from the training set was used for NTCP modeling. In this study, the LKB-NTCP value of a particular radiation-related adverse reaction manifesting in a specific OAR was calculated by 10^{-14} :

$$NTCP = \frac{1}{\sqrt{2\pi}} \int_{-\infty}^{t} \exp\left(\frac{-x^2}{2}\right) dx \tag{1}$$

while

$$t = \frac{EUD - TD_{50}*(DMF_1^{Y_1})*...*(DMF_K^{Y_k})}{m*TD_{50}*(DMF_1^{Y_1})*...*(DMF_K^{Y_k})}$$
(2)

and

$$EUD = \left(\sum_{i} \nu_{i} D_{i} \frac{1}{n}\right)^{n} \tag{3}$$

in which TD50 is the tolerance dose in Gy of the OAR that causes 50% complication risk, n describes the volume effect specific to the OAR of interest (varying from 0 to 1 as the volume effect increases), ¹⁵ and m represents the slope of the modeling curve at TD50 ranging between 0 and 1. Meanwhile, the influence of each risk or protective factor K corresponds to a parameter DMF_k that affects $TD50^{11}$ ($Y_k = 1$ if the patient meets factor K, and 0 if not).

Equation (3) describes the equivalent uniform dose (EUD)¹⁶ by performing an exponentially weighted summation of pairs of relative volume (vi) receiving a dose of Di, which can be derived from the differential DVH data of the related OAR.

The optimal values of key parameters (*TD50*, *n*, *m* and *DMFs*) were determined by maximum likelihood estimation at the maximum value of a log-likelihood (LL) function expressed as:

$$LL(n, m, TD50, DMFs)$$

$$= \sum_{j} (\ln NTCP_{j}(n, m, TD50, DMFs)^{Rj} + \ln(1 - NTCP_{j}(n, m, TD50, DMFs))^{1-Rj})$$
(4)

For patient j, if follow-up indicates grade 1 or higher RILI, then Rj=1; otherwise, Rj=0. The 95% confidence intervals (CI) of the optimal parameter values were determined with the profile likelihood method.¹⁰

Statistical analysis

In the training set, least absolute shrinkage and selection operator (LASSO) regression followed by univariate and multivariate logistic regressions were conducted to identify the independent risk factors for RILI, which would then be introduced into the LKB-NTCP model as DMFs. All relevant data analyses were performed with R version 4.3.1.

NTCP modeling was completed with self-written code in MATLAB (version R2021a, MathWorks, Inc). Subsequent model validations were done with R version 4.3.1.

The NTCP model was evaluated in both the training and testing sets to validate the model performance in similar populations that can be extrapolated. Overall performance was measured by Nagelkerke's R^2 and the Brier score. Nagelkerke's R^2 indicates the proportion of variance explained by the model. The Brier score measures the accuracy of the model's probabilistic predictions against actual binary outcomes. Discrimination was evaluated using the area under the receiver operating curve (AUC). To assess the calibration of the model, we performed the Hosmer-Lemeshow test, which compares the observed and expected outcomes, with a lower chi-square value and a P value greater than 0.05 indicating good model fit.

Relationship between $\Delta NTCP$ and thoracic anatomic features

Patient enrollment and treatment planning

Forty-five left-sided and thirty-five right-sided post-mastectomy BC patients who received conventional fractionated IMRT (50Gy/25Fx) were randomly selected from the original dataset and underwent PT planning at a prescription dose of 50 Gy_{RBE}/25Fx. The clinical target volumes (CTVs) for PT were consistent with those in the photon plans, including chest wall and regional lymph nodes (supraclavicular

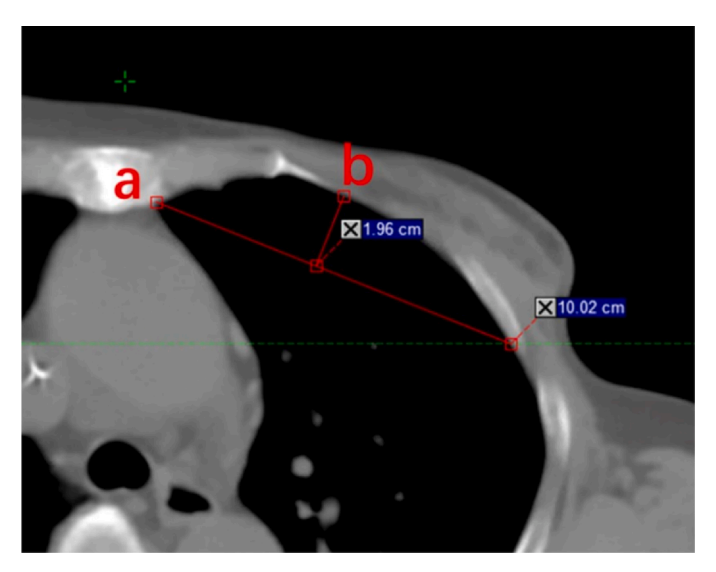


Figure 1. Illustration of the base length (a) and the arc height (b).

 \pm internal mammary lymph node \pm level 1-3 axillary lymph nodes). The target volumes were contoured as per the RADCOMP breast contouring atlas (v.3). The intensity-modulated proton therapy (IMPT) plans were created using RayStation treatment planning system (Version: 10B, RaySearch Laboratories, Sweden). Two co-planar beams were configured: one anterior-posterior (0°) beam and the other is an en-face beam perpendicular to the breast/chest-wall surface. The enface beam was positioned at mainly 45° for left-sided cases and 315° for right-sided cases. A range shifter with a water-equivalent thickness of 4.6 g/cm² was adopted for both beams. All plans were robustly optimized, accounting for 3 mm setup uncertainty and 3.5% range uncertainty. Dose calculation was performed using the Monte Carlo algorithm, assuming a constant relative biological effectiveness (RBE) value of 1.1. The plan normalization was set to cover 95% of CTV with 100% prescription dose. All proton plans were reviewed and approved by a senior radiation oncologist to ensure that the target volume coverage was clinically acceptable and comparable to that of the photon plans. The OAR delineation and dose constraints were provided in Supplementary Table 1.

Data collection for $\Delta NTCP$ and anatomic features

The $\Delta NTCP$ between photon and proton plans (defined as photon NTCP minus proton NTCP) of these patients were calculated with the corresponding baseline information and DVH data using the obtained NTCP model for RILI.

The anatomical features were quantified on planning CT in 6 parameters: the minimum thickness of remaining chest wall soft tissues across all the transverse planes on CT scans, ipsilateral lung volume, the ratio of anterior-posterior (AP) to left-right (LR) distance of thorax, the ratio of AP to LR distance of ipsilateral lung, the ratio of AP distance of thorax to AP distance of ipsilateral lung, and the Arc Height to Base Ratio (AHBR) (defined by the ratio of height to base of the arc formed by the osseous thorax within the parasternal to mid-axillary line range) (Figure 1). The last 4 parameters were measured at the transverse plane where the sternal angle and the fourth rib lies, respectively.

Statistical analysis

For anatomical features that followed a normal distribution, the Pearson correlation coefficient was used to measure their correlation with $\Delta NTCP$. Spearman rank correlation coefficient was applied for others. For anatomical features that showed significant results in the analysis, linear regression was further employed to investigate the strength and direction of the correlation.

Table 1
Cut-off points for continuous variables to be transversed to logical variables.

Cut-off value	Youden Index	Sensitivity	Specificity
52.50	0.224	0.622	0.602
23.52	0.157	0.526	0.632
172.50	0.133	0.774	0.359
20.50	0.116	0.675	0.442
	value 52.50 23.52 172.50	value Index 52.50 0.224 23.52 0.157 172.50 0.133	value Index 52.50 0.224 0.622 23.52 0.157 0.526 172.50 0.133 0.774

Abbreviations: BMI, body mass index, ISR, interval between surgery and radiotherapy, ICR, interval between chemotherapy and radiotherapy.

All statistical analyses were conducted using GraphPad Prism 10.1.0 software.

Results

The NTCP model generation

Independent prognostic factors for RILI

Of the 409 cases studied, 191(46.70%) patients experienced grade 1 or higher RILI. In the training set and testing set, there were 156/327(47.71%) and 35/82(42.68%) patients with positive outcomes, respectively (P = .415).

Search of independent prognostic factors for RILI was based on the training set data. Restricted by the aforementioned NTCP model formulas, some baseline characteristics were converted from continuous variables to logical variables according to the cut-off values determined with the receiver operating curve (ROC), as shown in Table 1. Full details of the patient and treatment characteristics to be candidates of prognostic factors for RILI are provided elsewhere (Supplementary Table 2).

In LASSO regression, when the regularization strength (λ) was set to the value of 0.0277 which achieving the lowest cross-validation error (λ minutes), 7 of the 19 variables were excluded with coefficients shrunk to zero (Supplementary Figure 1 and Table 3).

The remaining 12 logical variables (Age ≥ 53 years, Postmenopausal, Body mass index (BMI) $\geq 23.52\, kg/m^2$, Hyperlipidemia, Pulmonary primary disease, Mastectomy, Chemotherapy with anthracycline, Chemotherapy with taxane, HER2-targeted therapy, Interval between surgery and radiotherapy $\leq 172 days$, Interval between last cycle of chemotherapy and radiotherapy (ICR) $\leq 20 days$, Endocrine therapy before/during radiotherapy) were then included in the logistic regression

 Table 2

 Results of the univariate and multivariate logistic regression analysis about RILI.

	Univariate logistic regression		Multivariate logistic regression			
	Estimate	95%CI	P value	Estimate	95%CI	P value
Age ≥ 53 y	0.912	0.470 to 1.362	< .001	0.682	-0.342 to 1.735	.192
Post-menopausal	0.871	0.428 to 1.320	< .001	0.252	-0.808 to 1.285	.633
BMI $\geq 23.52 \mathrm{kg/m^2}$	0.642	0.202 to 1.087	.004	0.480	0.001 to 0.961	.049
Hyperlipidemia	-1.030	-2.960 to 0.455	.212			
Pulmonary primary disease	0.871	0.131 to 1.664	.025	0.619	-0.195 to 1.480	.145
Mastectomy	0.511	0.025 to 1.006	.041	0.256	-0.273 to 0.790	.343
Chemotherapy with anthracycline	0.700	0.070 to 1.366	.033	0.560	-0.258 to 1.400	.184
Chemotherapy with taxane	0.910	-0.091 to 2.067	.091			
HER2-targeted therapy	0.483	0.008 to 0.963	.047	0.395	-0.124 to 0.919	.137
ISR ≤ 172 d	-0.651	-1.147 to -0.166	.009	-0.424	-1.055 to 0.194	.181
$ICR \le 20 d$	0.541	0.092 to 0.996	.019	0.605	0.125 to 1.092	.014
Endocrine therapy before/during radiotherapy	-1.041	-2.561 to 0.189	.123			

Abbreviations: BMI, body mass index; ISR, interval between surgery and radiotherapy; ICR, interval between chemotherapy and radiotherapy. 327 cases in the training set were included in this analysis.

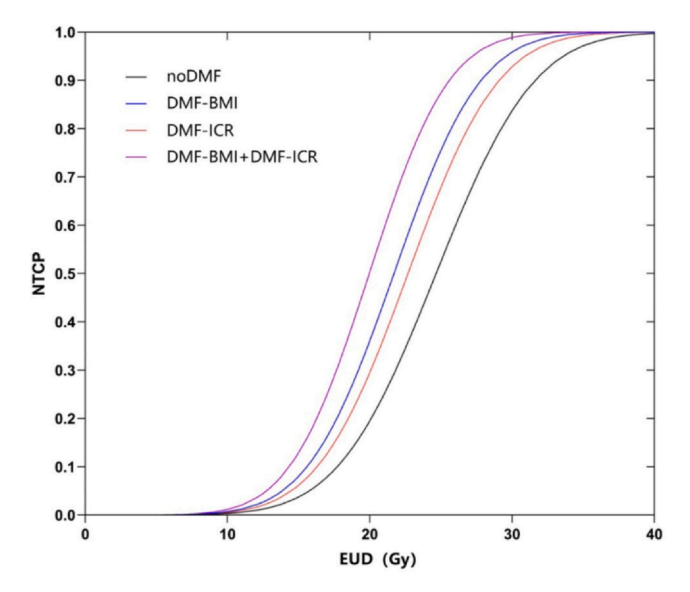


Figure 2. NTCP curve versus EUD corresponding to the LKB-NTCP model with DMFs $(n = 0.40, m = 0.21, TD50 = 24.66 \,\text{Gy}, DMF-ICR = 0.92, DMF-BMI = 0.88).$

(Table 2). The multivariate analysis suggested that: BMI $\geq 23.52\,\mathrm{kg/m^2}$ (regression coefficient 0.480, 95%CI 0.001-0.961; P=.049) and ICR ≤ 20 days (regression coefficient 0.605, 95%CI 0.125-1.092; P=.014) were independent risk factors for developing grade 1 or higher RILI within one year after radiotherapy in BC patients. These two factors were then introduced into the LKB-NTCP model as DMFs, represented by DMF-BMI and DMF-ICR.

NTCP model parameters and model performance

The maximum likelihood estimates of the LKB-NTCP model parameters were: n=0.40 (95%CI 0.374-0.419), m=0.22 (95%CI 0.171-0.287), TD50=24.66 Gy (95%CI 23.734-25.339), DMF-ICR=0.92 (95%CI 0.872-0.964), DMF-BMI=0.88 (95%CI 0.832-0.915).

Table 3Results of NTCP model validation.

Training set Testing set Internal validation (Median [Range]) AUC (95% CI) 0.754 (0.702-0.805) 0.733 (0.620-0.845) 0.755 [0.631-0.847] Brier score 0.201 0.209 0.198 [0.149-0.252] Nagelkerke's R2 0.256 $X^2 = 3.342 P = .911$ Hosmer-Lemeshow test $X^2 = 8.175 P = .417$

meets the risk factors for RILI represented by the DMFs, the NTCP value calculated for the same EUD value may fall on any of the corresponding curves in the graph.

The Nagelkerke's R^2 values of the model in the training and testing

The NTCP-EUD curves of the model corresponding to the optimal parameters are plotted in Figure 2. Depending on whether the patient

The Nagelkerke's R^2 values of the model in the training and testing set were 0.256 and 0.206, respectively, while the Brier scores were 0.201 and 0.209 (Table 3). The AUC was 0.754 (standard error 0.026, 95%CI 0.702-0.805) in the training set and 0.733 (standard error 0.057, 95%CI 0.620-0.845) in the testing set (Table 3). The Hosmer-Lemeshow test showed no significant difference between the observed outcomes and predicted risks in both the training (P = .911) and testing set (P = .417) (Table 3). In internal validation (Table 3), we got a median Brier score of 0.198 (range 0.149-0.252) and a median AUC of 0.755 (range 0.631-0.847). In the calibration plot of the whole dataset (including the training and testing set) (Supplementary Figure 2), the trend line of the NTCP model prediction versus the observation is close to the ideal line.

Relationship between anatomic factors and $\Delta NTCP$

Detailed patient characteristics of the cohort undergoing PT planning were presented in Supplementary Table 4. In dose comparison between proton and photon plans, PT demonstrated advantages in dose homogeneity within the target volume as well as in dose sparing of OARs, including the heart and ipsilateral lung (Supplementary Table 5).

The mean NTCP values of proton and photon plans were 9.36% (standard deviation (STD) 3.78%) and 66.81% (STD 13.05%), respectively. The NTCP values for proton plans were significantly reduced (Paired t test P < .0001) compared to photons, with a Δ NTCP of 57.45% (STD 10.51%).

The distribution of thoracic anatomical features is shown in Table 4, while the results of the correlation analysis are summarized in Table 5. At the transverse plane of the sternal angle on CT scans, AHBR was positively correlated with Δ NTCP (%) (Pearson correlation coefficient 0.220, 95%CI 0.001-0.420, P = 0.049). (For clarity, AHBR hereafter specifically indicates the measurement taken at the transverse plane of the

Table 4
Characteristics of anatomic features on CT scans.

	Mean (± STD)
At the transverse plane of sternal angle	
AP to LR ratio of thorax	$0.64 (\pm 0.06)$
AP to LR ratio of ipsilateral lung	$1.22 (\pm 0.12)$
Ratio of AP distance of thorax to AP distance of	$0.95 (\pm 0.03)$
ipsilateral lung	
AHBR ^a	$0.19 (\pm 0.04)$
At the transverse plane of the fourth rib	
AP to LR ratio of thorax	$0.68 (\pm 0.06)$
AP to LR ratio of ipsilateral lung	$1.31 (\pm 0.13)$
Ratio of AP distance of thorax to AP distance of	$0.98 (\pm 0.03)$
ipsilateral lung	
AHBR	$0.23 (\pm 0.03)$
Across all transverse planes	
Volume of the ipsilateral lung, cm ³	1186.41 (± 240.24)
*Minimum thickness of remaining chest wall soft tissues, cm	0.47 (± 0.23)

Abbreviations: AP, anterior-posterior, LR left-right, AHBR arc height to base ratio

sternal angle, unless explicitly noted.) Subsequent linear regression on AHBR to Δ NTCP yielded a regression coefficient of 56.560 (standard error 28.380, $R^2 = 0.048$, P = .049) (Supplementary Figure 3).

Discussion

As the first step of this study, we developed a DMF-cooperated LKB-NTCP model to predict the risk of grade 1 or higher RILI within 1 year after radiotherapy in BC patients. The model showed good performance both in training and testing sets, indicating a consistency in its robustness. It also achieved a higher AUC value than models from other studies with similar endpoints (0.733 vs 0.702 (Zhou et al 17) and 0.703 (Rancati et al 18), P = .002 for both) in the testing set.

Among the optimal parameters of our NTCP model for RILI, the value of n (0.40) has drawn our attention, as it indicates a relatively smaller volume effect of lungs than those reported in previous lung toxicity NTCP models (n ranging from 0.9 to 1).^{17–19} However, it is supported by Tucker et al,²⁰ who found that an NTCP model with n = 0.41 better predicted radiation pneumonitis (RP) in non-small cell lung cancer patients than with n = 1. Their subsequent study²¹ also

confirmed that EUD calculated with n = 0.5 predicted RP risk more accurately than mean lung dose (equals EUD calculated with n = 1).

While the dosimetric advantage of PT in sparing key OARs—such as the heart and lungs—has been well established and confirmed in our study (Supplementary Table 5), the benefit varies across individual patients, which may serve as a valuable basis for patient selection. With a same technical platform, the dose-sparing benefit, however, may be attributed to thoracic anatomical variations.

For example, cardiac contact distance 22 (defined as the maximum length of contact between the heart and chest wall on the left side of the sternum) and heart volume in field 23,24 (defined as the heart volume encompassed by the 50% isodose line) can predict the benefit from the deep-inspiration breath-hold (DIBH) technique using 3-dimensional conformal radiotherapy. Thus, we explored factors that potentially influence the benefits of PT (Δ NTCP) in terms of thoracic anatomical characteristics based on the NTCP model for RILI. In the correlation analysis, AHBR at the transverse plane of the sternal angle showed a significant positive correlation with Δ NTCP (%) between proton and photon plans (P = 0.049). Subsequent linear regression indicates that for every 0.1 increase in this ratio, Δ NTCP increases by 5.656%.

With the "Bragg Peak,"²⁵ IMPT can narrow the low-to-intermediate dose region so as to be better conformal to the target volume. As shown in Figure 3, the 50% isodose line at the sternal angle plane of the proton plan better matches the contour of the target area and spares most of the lung tissue irradiated in the photon plan.

While the parasternal and mid-axillary lines are usually considered the inner and outer boundaries of the CTV delineation for breast/chestwall irradiation, AHBR aims to reflect the convexity of the arc formed by the osseous thorax within that range. Comparing the 50% isodose lines of patient A and B (Figure 3), it can be proposed that a more convex target volume (indicating a more convex osseous thorax as in Figure 3A), which is an unfavorable anatomy associated with increased lung dose-volume when photon radiotherapy is to be given, will lead to higher magnitude of lung sparing in proton plans. It aligns with our conclusion that a larger AHBR correlates with greater advantage in lung sparing for protons. However, AHBR at the fourth rib level did not demonstrate significant correlation with ANTCP. Patients receiving regional nodes irradiation are associated with higher ipsilateral lung dose. 26,27 As most of the regional nodes situated above the fourth-intercostal space, the spared lung volume in proton plans at a more cephalad level (eg, the sternal angle level compared to the fourth rib level in this study) may have greater influence on the ipsilateral lung irradiation and NTCP prediction.

We further tried to explore the potential correlation between the cardiac and pulmonary sparing benefits of PT. The risk of ACE for all 80 patients in photon and proton plans (estimated based on the work of

Table 5 Correlation analysis between anatomical features and Δ NTCP.

	Correlation coefficient (95%CI)	R^2	P value
At the transverse plane of sternal angle			
AP to LR ratio of thorax	0.047 (-0.175 to 0.264)	0.002	.681
AP to LR ratio of ipsilateral lung	-0.023 (-0.242 to 0.197)	0.001	.837
Ratio of AP distance of thorax to AP distance of ipsilateral lung	-0.125 (-0.336 to 0.097)	0.016	.268
AHBR	0.220 (0.001 to 0.420)	0.048	.049
At the transverse plane of the fourth rib			
AP to LR ratio of thorax	0.101 (-0.121 to 0.314)	0.010	.373
AP to LR ratio of ipsilateral lung	0.038 (-0.183 to 0.256)	0.001	.738
Ratio of AP distance of thorax to AP distance of ipsilateral lung	0.145 (-0.077 to 0.354)	0.021	.198
AHBR	0.175 (-0.046 to 0.380)	0.031	.120
Across all transverse planes			
Volume of the ipsilateral lung, cm ³	-0.163 (-0.379 to 0.059)	0.027	.148
*Minimum thickness of remaining chest wall soft tissues, cm	0.169 (-0.059 to 0.380)	/	.134

Abbreviations: AP, anterior-posterior; LR, left-right; AHBR, arc height to base ratio.

^a *AHBR*: the ratio of height to base of the arc formed by the osseous thorax within the parasternal to mid-axillary line range (Figure 1).

^{*} Variable marked with "*" did not follow a normal distribution and was otherwise presented by median(range) as: Minimum thickness of remaining chest wall soft tissues, 0.42 (0.24-1.90) cm.

^{*} Correlation between anatomical features and ΔNTCP was analyzed with the Pearson correlation coefficient, except for features marked with "*" of which correlation with ΔNTCP was tested with the Spearman rank correlation coefficient for not following a normal distribution.

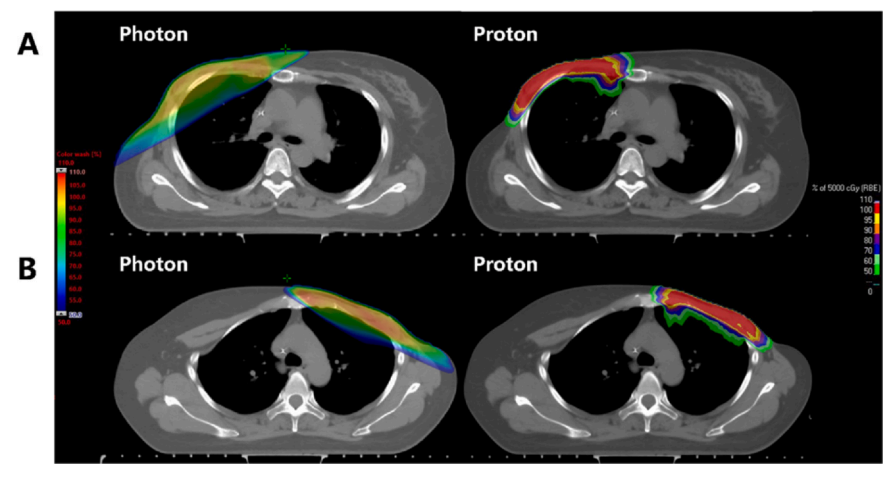


Figure 3. Fifty percent isodose lines at the transverse plane of the sternal angle in photon and proton plans for patient A (A) and B (B). Compared to patient A (A), patient B (B) held a flatter osseous thorax, and the proton plan for her showed less advantage in lung sparing.

Boersma et al⁵), along with the NTCP values for RILI, was summarized in Supplementary Table 6. Pearson correlation analysis revealed no significant association between the Δ NTCP values for ACE and RILI (P=.146). The extent of benefit for heart and lung did not seem to increase proportionally, which may be attributed to their different anatomical features for corresponding dose sparing potential with IMPT.

One critical limitation of the current study is the endpoint set for our NTCP model (grade ≥ 1 RILI), which holds limited clinical significance. Despite our awareness, the positive cases of grade ≥2 RILI in our cohort were insufficient (2 out of 409) to support the NTCP modeling. However, radiological changes may be the earliest manifestation of more severe complications. Studies by Lind et al.28 and Bhadra et al.29 have demonstrated that among patients with grade 1 RILI, those exhibiting moderate-to-severe radiological reactions—classified according to Arriagada's system, 30 which categorizes CT responses based on changes in density—were more likely to develop respiratory symptoms or experience greater reductions in lung capacity. With limited cases of grade ≥2 events, further study may refine the classification of grade 1 RILI to better define the extent of radiological lung injury and to improve the clinical impact of the endpoint. In addition, in the context of multimodal BC treatment, it is important to minimize even grade 1 RILI to reduce cumulative toxicity. Several novel systemic therapies in international guidelines, such as CDK4/6 inhibitors, 31,32 ADCs^{33,34} and PARP inhibitors³⁵ have been reported to be associated with lung toxicity. To maximize lung sparing is thus associated with an increasing clinical impact under this context.

In this study, the probability of RILI following PT was predicted by the same LKB-NTCP model generated with photon-based data. Blanchard et al³⁶ verified that the accuracy of the NTCP model derived from photon therapy data might decrease in proton treatment for head and neck cancer patients even though the deviation was within an acceptable range. Thus, we tend to believe that the loss of accuracy as using photon-based NTCP model on proton irradiation is unlikely to significantly impact the related conclusions. Nevertheless, future efforts should focus on developing NTCP models specifically for PT to improve the preciseness. Also, given that both the training and testing sets originated from the same institutional population, the performance of our NTCP model warrants further validation in external datasets.

Based on previous research, RBE varies along the Bragg Peak and may reach an average of 1.35 at the distal end of the Spread-Out Bragg Peak, 37 which anatomically adjacent to the ribs and the anterior portion of ipsilateral lung. Ödén et al 38 reported that in proton plans of BC, pulmonary doses calculated using a variable RBE model (incorporating linear energy transfer and α/β ratios) were higher compared to those calculated with a fixed RBE of 1.1. It is possibly that our study

underestimates the lung dose and the associated risk of RILI in NTCP assessment for PT, as a constant RBE of 1.1 was applied.

It should be acknowledged that the correlation between AHBR and Δ NTCP was modest, as reflected by the low R^2 value (0.048). Besides, when IMRT plans were separately analyzed, there exists a trend with no statistical difference towards AHBR and NTCP-RILI values, P value (P = .084). Moreover, as all dosimetry data were carried out on freebreathing planning CT, the influence of breathing conditions warrants further investigation. Previous studies^{39,40} have suggested that the DIBH technique can lead to sternal displacement and lung expansion, which could theoretically affect the AHBR measurement at the transverse plane of the sternal angle. To verify this assumption, we conducted a preliminary observation in another cohort of 18 DIBH-treated patients and found AHBR values was higher under DIBH than under free-breathing $(0.20 \pm 0.04 \text{ vs } 0.18 \pm 0.04, \text{ Paired } t \text{ test } P < .0001)$. Therefore, the feature "AHBR at the transverse plane of sternal angle" points toward a potentially valuable direction for further investigation, rather than representing a definitive conclusion suitable for immediate clinical translation. To confirm its clinical relevance, further validation in larger and more diverse cohorts, such as those undergoing DIBH, is necessary. The incorporation of radiomics-based approaches may facilitate a more comprehensive exploration of thoracic anatomical variables.

As an extension, when investigating the benefits of PT, it is also important to integrate potential adverse effects beyond RILI and cardiac toxicity, such as skin toxicities, ⁴¹ rib fracture ⁴² and capsular contracture in reconstructed breasts. ⁴³ Retrospective studies ^{41,44} have reported an increased risk of radiation dermatitis in BC patients receiving PT, which has been attributed, at least in part, to the use of passive scattering proton beams. In the study by Hsieh et al, ⁴⁵ the proton and photon plans exhibited comparable skin dosimetry; however, the incidence of radiation dermatitis remained higher with PBS PT than with photons, highlighting the value of establishing corresponding modeling ⁴⁶ to increase the precision of PT-related skin toxicity evaluation. The same applies to other PT-related concerns mentioned above.

Conclusion

Patients with BMI $\geq 23.52\,kg/m^2$ or ICR $\leq 20\,days$ are at higher risk of developing RILI. Thoracic anatomical features such as larger AHBR at the transverse plane of the sternal angle on planning CT was found to be a potential parameter for quick selection of BC patients potentially benefit more from PT in terms of lung sparing. Our study provides a possibly solution in the recommendation of PT without double planning. Continuous efforts should be made not only to validate this finding but also to develop a more integrated predictive approaches with practical guidance in patient selection.

Ethics statement

All procedures were performed in compliance with relevant laws and institutional guidelines and have been approved by the appropriate institutional committees. The ethical approvals obtained were: NCT03829553, reference number: 2018-95-3, date: 2021.1.21; NCT02942615, reference number: 2016-101, date: 2016-10-26.

Funding

This study was supported in part by the Shanghai Science and Technology Innovation Action Plan (grant number 23Y41900100), the National Key Research and Development Program of China (grant number 2022YFC2404602), the Shanghai Hospital Development Center Foundation (grant number SHDC12023108), the Scientific and Technological Innovation Action Plan of the Shanghai Science and Technology Committee (grant number 22Y31900103), the Clinical Research of the Shanghai Municipal Health Commission (grant number 20224Y0025), the Beijing Science and Technology Innovation Medical Development Foundation (grant number KC2021-JX-0170-9), and the National Natural Science Foundation of China (grant number 82373514, 82373202, and 81972963).

CRediT authorship contribution statement

Xiao-Yu Wu: Writing- Original draft preparation, Formal analysis, Software, Validation. Mei Chen: Writing- Original draft preparation, Methodology, Validation. Gang Cai: Writing- Reviewing and Editing, Resources, Validation. Rong Cai: Writing- Reviewing and Editing, Resources. Cheng Xu: Writing- Reviewing and Editing, Resources. Dan Ou: Writing- Reviewing and Editing, Resources, Data curation. Fei-Fei Xu: Writing- Reviewing and Editing, Resources, Data curation. Yu-Jie Wang: Writing- Reviewing and Editing, Conceptualization. Huan Li: Writing- Reviewing and Editing, Conceptualization. Min Li: Writing-Reviewing and Editing, Data curation. Yi-Bin Zhang: Writing-Reviewing and Editing, Resources, Data curation. Lu Cao: Writing-Reviewing and Editing, Conceptualization, Visualization. Jia-Yi Chen: Writing- Reviewing and Editing, Resources, Conceptualization, Supervision.

Declaration of Conflicts of Interest

The authors declare that they have no known competing financial interests or personal relationships that could have appeared to influence the work reported in this paper.

Data Availability Statement

Research data are stored in an institutional repository and will be shared upon request to the corresponding author.

Acknowledgments

This work was previously presented at the American Society for Radiation Oncology's (ASTRO) 66th Annual Meeting, conducted September 29-October 2, 2024, in Washington, D.C.

Appendix A. Supporting Information

Supplementary data associated with this article can be found in the online version at doi:10.1016/j.ijpt.2025.101196.

References

 Wu XY, Chen M, Cao L, Li M, Chen JY. Proton therapy in breast cancer: a review of potential approaches for patient selection. *Technol Cancer Res Treat*. 2024;23:15330338241234788. https://doi.org/10.1177/15330338241234788

- Langendijk JA, Lambin P, De Ruysscher D, et al. Selection of patients for radiotherapy with protons aiming at reduction of side effects: the model-based approach. *Radiother Oncol.* 2013;107(3):267–273.
- Langendijk JA, Boersma LJ, Rasch CRN, et al. Clinical trial strategies to compare protons with photons. Semin Radiat Oncol. 2018;28(2):79–87.
- Tambas M, Steenbakkers RJHM, van der Laan HP, et al. First experience with modelbased selection of head and neck cancer patients for proton therapy. *Radiother Oncol*. 2020:151:206–213.
- Boersma LJ, Sattler MGA, Maduro JH, et al. Model-based selection for proton therapy in breast cancer: development of the national indication protocol for proton therapy and first clinical experiences. Clin Oncol (R Coll Radiol). 2022;34(4):247–257.
- Darby SC, Ewertz M, McGale P, et al. Risk of ischemic heart disease in women after radiotherapy for breast cancer. N Engl J Med. 2013;368(11):987–998.
- Stahl JM, Hong JC, Lester-Coll NH, et al. Chest wall deformity in the radiation oncology clinic. Anticancer Res. 2016;36(10):5295–5300.
- Borst GR, Ishikawa M, Nijkamp J, et al. Radiation pneumonitis after hypofractionated radiotherapy: evaluation of the LQ(L) model and different dose parameters. Int J Radiat Oncol Biol Phys. 2010;77(5):1596–1603.
- Common Terminology Criteria for Adverse Events (CTCAE) 2017. https://ctep. cancer.gov/protocolDevelopment/electronic_applications/docs/CTCAE_v5_Quick_ Reference 5 × 7.ndf.
- Wang Z, Chen M, Sun J, et al. Lyman-Kutcher-Burman normal tissue complication probability modeling for radiation-induced esophagitis in non-small cell lung cancer patients receiving proton radiotherapy. *Radiother Oncol.* 2020;146:200–204. https://doi.org/10.1016/j.radonc.2020.03.003
- Tucker SL, Liu HH, Liao Z, et al. Analysis of radiation pneumonitis risk using a generalized Lyman model [published correction appears in Int J Radiat Oncol Biol Phys. 2010 Sep 1;78(1):316-7. Int J Radiat Oncol Biol Phys. 2008;72(2):568-574.
- Lyman JT. Complication probability as assessed from dose-volume histograms. Radiat Res Suppl. 1985;8:S13–S19.
- Kutcher GJ, Burman C. Calculation of complication probability factors for non-uniform normal tissue irradiation: the effective volume method. *Int J Radiat Oncol Biol Phys.* 1989;16(6):1623–1630.
- Kutcher GJ, Burman C, Brewster L, et al. Histogram reduction method for calculating complication probabilities for three-dimensional treatment planning evaluations. *Int* J Radiat Oncol Biol Phys. 1991;21(1):137–146.
- Gay HA, Niemierko A. A free program for calculating EUD-based NTCP and TCP in external beam radiotherapy. *Phys Med.* 2007;23(3-4):115–125. https://doi.org/10. 1016/j.ejmp.2007.07.001
- Niemierko A. Reporting and analyzing dose distributions: a concept of equivalent uniform dose. Med Phys. 1997;24(1):103–110.
- Zhou ZR, Han Q, Liang SX, et al. Dosimetric factors and Lyman normal-tissue complication modelling analysis for predicting radiation-induced lung injury in postoperative breast cancer radiotherapy: a prospective study. Oncotarget. 2017;8(20):33855–33863
- Rancati T, Wennberg B, Lind P, et al. Early clinical and radiological pulmonary complications following breast cancer radiation therapy: NTCP fit with four different models. Radiother Oncol. 2007;82(3):308–316.
- Seppenwoolde Y, Lebesque JV, de Jaeger K, et al. Comparing different NTCP models that predict the incidence of radiation pneumonitis. Normal tissue complication probability. Int J Radiat Oncol Biol Phys. 2003;55(3):724–735.
- Tucker SL, Mohan R, Liengsawangwong R, et al. Predicting pneumonitis risk: a dosimetric alternative to mean lung dose. Int J Radiat Oncol Biol Phys. 2013;85(2):522–527.
- Tucker SL, Xu T, Paganetti H, et al. Validation of effective dose as a better predictor
 of radiation pneumonitis risk than mean lung dose: secondary analysis of a randomized trial. Int J Radiat Oncol Biol Phys. 2019;103(2):403–410.
- Czeremszyńska B, Drozda S, Górzyński M, Kępka L. Selection of patients with left breast cancer for deep-inspiration breath-hold radiotherapy technique: results of a prospective study. Rep Pract Oncol Radiother. 2017;22(5):341–348. https://doi.org/ 10.1016/j.por.2017.05.002
- Register S, Takita C, Reis I, Zhao W, Amestoy W, Wright J. Deep inspiration breath-hold technique for left-sided breast cancer: an analysis of predictors for organ-at-risk sparing. *Med Dosim.* 2015;40(1):89–95. https://doi.org/10.1016/j.meddos.2014.10.005
- 24. Ferdinand S, Mondal M, Mallik S, et al. Dosimetric analysis of deep inspiratory breath-hold technique (DIBH) in left-sided breast cancer radiotherapy and evaluation of pre-treatment predictors of cardiac doses for guiding patient selection for DIBH. Tech Innov Patient Support Radiat Oncol. 2021;17:25–31. https://doi.org/10.1016/j.tipsro.2021.02.006 Published 2021 Mar 1.
- Newhauser WD, Zhang R. The physics of proton therapy. Phys Med Biol. 2015;60(8):R155–R209.
- Aznar MC, Duane FK, Darby SC, et al. Exposure of the lungs in breast cancer radiotherapy: a systematic review of lung doses published 2010-2015. Radiother Oncol. 2018;126(1):148–154.
- Finazzi T, Nguyen VT, Zimmermann F, et al. Impact of patient and treatment characteristics on heart and lung dose in adjuvant radiotherapy for left-sided breast cancer. Radiat Oncol. 2019;14(1):153.
- 28. Lind PA, Svane G, Gagliardi G, et al. Abnormalities by pulmonary regions studied with computer tomography following local or local-regional radiotherapy for breast cancer. Int J Radiat Oncol Biol Phys. 1999;43(3):489–496.
- Bhadra K, Patra NB, Manna A, et al. Abnormalities by pulmonary regions studied with computer tomography and clinical correlation following local-regional radiotherapy for breast cancer. South Asian J Cancer. 2013;2(1):21–25.
- Arriagada R, de Guevara JC, Mouriesse H, et al. Limited small cell lung cancer treated by combined radiotherapy and chemotherapy: evaluation of a grading system of lung fibrosis. Radiother Oncol. 1989;14(1):1–8.

- Rajendran A, Kunoor A, Pushpa Ragahavan R, Keechilat P. Ribociclib-associated organising pneumonia. BMJ Case Rep. 2021;14(12):e245187. https://doi.org/10. 1136/bcr-2021-245187 Published 2021 Dec 20.
- Okayasu K, Kawasaki T, Kumagai J, Miyazaki Y. Clinicoradiological course of abemaciclib-induced pneumonitis with histology findings. *BMJ Case Rep.* 2023;16(5):e254349. https://doi.org/10.1136/bcr-2022-254349 Published 2023 May 2.
- LaMorte D, Desmond D, Ellis J, Lipkowitz S. Acute eosinophilic pneumonia: a fatal reaction to ado-trastuzumab. *BMJ Case Rep.* 2021;14(9):e243881. https://doi.org/ 10.1136/bcr-2021-243881 Published 2021 Sep 3.
- Swain SM, Nishino M, Lancaster LH, et al. Multidisciplinary clinical guidance on trastuzumab deruxtecan (T-DXd)-related interstitial lung disease/pneumonitis-focus on proactive monitoring, diagnosis, and management. *Cancer Treat Rev.* 2022;106:102378. https://doi.org/10.1016/j.ctrv.2022.102378
- Shu Y, He X, Liu Y, Wu P, Zhang Q. A real-world disproportionality analysis of olaparib: data mining of the public version of FDA Adverse Event Reporting System. Clin Epidemiol. 2022;14:789–802. https://doi.org/10.2147/CLEP.S365513 Published 2022 Jun 28.
- Blanchard P, Wong AJ, Gunn GB, et al. Toward a model-based patient selection strategy for proton therapy: external validation of photon-derived normal tissue complication probability models in a head and neck proton therapy cohort. *Radiother Oncol.* 2016;121(3):381–386.
- Paganetti H, Blakely E, Carabe-Fernandez A, et al. Report of the AAPM TG-256 on the relative biological effectiveness of proton beams in radiation therapy. *Med Phys.* 2019;46(3):e53–e78. https://doi.org/10.1002/mp.13390
- Ödén J, Toma-Dasu I, Eriksson K, Flejmer AM, Dasu A. The influence of breathing motion and a variable relative biological effectiveness in proton therapy of left-sided breast cancer. Acta Oncol. 2017;56(11):1428–1436. https://doi.org/10.1080/ 0284186X.2017.1348625

- Kim T, Reardon K, Trifiletti DM, et al. How dose sparing of cardiac structures correlates with in-field heart volume and sternal displacement. *J Appl Clin Med Phys*. 2016;17(6):60–68. https://doi.org/10.1120/jacmp.v17i6.6324 Published 2016 Nov 8.
- Oechsner M, Düsberg M, Borm KJ, Combs SE, Wilkens JJ, Duma MN. Deep inspiration breath-hold for left-sided breast irradiation: analysis of dose-mass histograms and the impact of lung expansion. *Radiat Oncol.* 2019;14(1):109. https://doi.org/10.1186/s13014-019-1293-1 Published 2019 Jun 18.
- DeCesaris CM, Rice SR, Bentzen SM, Jatczak J, Mishra MV, Nichols EM.
 Quantification of acute skin toxicities in patients with breast cancer undergoing
 adjuvant proton versus photon radiation therapy: a single institutional experience.
 Int J Radiat Oncol Biol Phys. 2019;104(5):1084–1090. https://doi.org/10.1016/j.
 iiroba 2019.04.015
- Bradley JA, Liang X, Mailhot Vega RB, et al. Incidence of Rib fracture following treatment with proton therapy for breast cancer. *Int J Part Ther.* 2023;9(4):269–278. https://doi.org/10.14338/IJPT-22-00034.1 Published 2023 Mar 24.
- Mutter RW, Giri S, Fruth BF, et al. Conventional versus hypofractionated postmastectomy proton radiotherapy in the USA (MC1631): a randomised phase 2 trial. *Lancet Oncol*. 2023;24(10):1083–1093. https://doi.org/10.1016/S1470-2045(23)00388-1
- 44. Galland-Girodet S, Pashtan I, MacDonald SM, et al. Long-term cosmetic outcomes and toxicities of proton beam therapy compared with photon-based 3-dimensional conformal accelerated partial-breast irradiation: a phase 1 trial. *Int J Radiat Oncol Biol Phys.* 2014;90(3):493–500.
- Hsieh CC, Yu CC, Chu CH, Chen WC, Chen MF. Radiation-induced skin and heart toxicity in patients with breast cancer treated with adjuvant proton radiotherapy: a comparison with photon radiotherapy. Am J Cancer Res. 2023;13(10):4783–4793 Published 2023 Oct 15.
- Palma G, Monti S, Conson M, et al. NTCP models for severe radiation induced dermatitis after IMRT or proton therapy for thoracic cancer patients. Front Oncol. 2020;10:344. https://doi.org/10.3389/fonc.2020.00344 Published 2020 Mar 17.